

Model of Electron Collecting Plasma Contactors

V. A. Davis,* I. Katz,† M. J. Mandell,‡ and D. E. Parks§

S-CUBED Division of Maxwell Laboratories, Inc., La Jolla, California 92038

In laboratory experiments, plasma contactors are observed to collect ampere-level electron currents with low impedance. In order to extend the laboratory experience to the low-Earth-orbit environment, a model of plasma contactors is being developed. Laboratory results are being used to support and validate the model development. The important physical processes observed in the laboratory are that the source plasma is separated from the background plasma by a double layer and that ionization of the expellant gas by the collected electrons creates the bulk of the ions that leave the source plasma. The model, which uses Poisson's equation with a physical charge density that includes the ion and electron components of both the source and the ambient plasmas, reproduces this phenomenon for typical experimental parameters. The calculations, in agreement with the laboratory results, show little convergence of the accelerated electrons. The angular momentum of the incoming electrons dramatically reduces the peak electron density. These electrons ionize enough gas to generate the source plasma. Calculations show that the increase in ionization rate with potential produces a steep rise in collected current with increasing potential as seen in the laboratory.

Nomenclature

| | |
|----------------|---|
| a | = average double-layer radius |
| E | = kinetic energy of ions from source |
| E_1 | = initial kinetic energy of ions created by ionization |
| e | = electron charge |
| I_i | = current of ions flowing outward |
| I_o | = current of electrons flowing inward |
| m_{hc} | = mass of ions flowing outward |
| \dot{n} | = rate of neutrals leaving the source |
| n_e | = number density of accelerated electrons |
| n_{es} | = number density of source electrons |
| n_{es}^o | = number density of source electrons at $\phi = \theta_{ln}2$ |
| n_i^o | = number density of source ions at r_{min} |
| n_{is} | = number density of ions emitted by the source |
| n_{iz} | = number density of ions created by ionization |
| \dot{n}_{iz} | = rate of ion creation due to ionization |
| n_n | = number of density of neutrals |
| n_{no} | = constant component of neutral number density |
| n_o | = number density of background or ambient plasma |
| r | = radial location |
| r | = location |
| r_i | = inner radius of double layer |
| r_{max} | = maximum radius of calculational space |
| r_{min} | = inner radius of calculational space |
| r_o | = outer radius of double layer |
| v_e | = velocity of accelerated electrons |
| v_n | = velocity of neutrals leaving the source |
| θ | = temperature of source electrons |
| θ_a | = temperature of background or ambient plasma |
| θ_n | = temperature of the neutral gas leaving the source |
| ρ | = total charge density |
| ρ_a | = charge density due to charge separation of the background or ambient plasma |
| σ | = ionization cross section |
| ϕ | = potential |
| ϕ_i | = potential at r_i |

| | |
|----------|---|
| ϕ_k | = potential of the anode (and keeper ring) |
| Ψ | = angle between the vector to location of interest and the line of axial symmetry |
| Ω | = solid angle of calculated space |

Introduction

IN laboratory plasma chambers, hollow-cathode-based plasma contactors are observed to both emit and collect ampere-level electron currents with low impedance.¹ On spacecraft, hollow cathodes and similar devices have dramatically reduced spacecraft charging during electron gun operations² and magnetospheric substorm events.³ The laboratory behavior¹ of hollow-cathode-based plasma contactors and the limited space experience^{2,3} with hollow cathodes suggest that a hollow-cathode-based plasma contactor is the ideal device to provide electrical connection with the space plasma for many applications. What makes hollow-cathode-based plasma contactors particularly useful is that the same device can both emit and collect electrons. An application for which a hollow-cathode-based plasma contactor is well suited is at both ends of an electrodynamic tether such as TSS-1 (tethered satellite system 1) or OTEP (orbital tether electrodynamic platform).⁴ The present work discusses plasma contactors only in the electron collection mode.

A hollow-cathode-based plasma contactor is a plasma source that emits neutral atoms, ions, and electrons. In the laboratory, as shown in Fig. 1, a high-density plasma cloud is formed near the potential of the source, which is on the order of 20–100 V^{1,5–7} above the potential of the surrounding

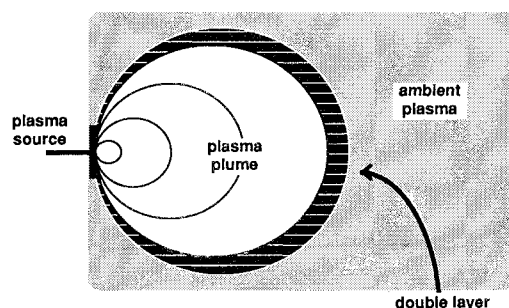


Fig. 1 Plasma in the vicinity of a hollow-cathode-based plasma contactor in the laboratory.

Received Oct. 6, 1989; revision received April 17, 1990; accepted for publication May 25, 1990. Copyright © 1990 by the American Institute of Aeronautics and Astronautics, Inc. All rights reserved.

*Staff Scientist. Member AIAA.

†Manager, Space Physics Program. Member AIAA.

‡Staff Scientist. Senior Member AIAA.

§Senior Research Scientist.

plasma. Background electrons are accelerated to the elevated potential and ionize the neutrals, generating more plasma. The presence of the high-density plasma serves to enlarge the sheath. As the collected current is roughly the thermal current times the sheath area, more current is collected for a given potential difference by the plasma-enlarged sheath.

The laboratory experiments have been done in a vacuum chamber with a simulator hollow cathode supplying the ambient plasma.⁵⁻⁷ The hollow-cathode-based plasma contactor that was being evaluated was at one end of the chamber and was collecting electrons on a 12-cm-diam anode plate. A Langmuir probe, an emissive probe, and a retarding potential analyzer were used to determine the plasma characteristics.

There is some concern as to the applicability of the results of the laboratory test tank experiments to the space environment. The major differences between the laboratory and space are due to the lower neutral density, plasma density, and plasma temperature of the ambient plasma in space. The lower ambient neutral density means that the source neutrals are the only neutrals available for ionization.¹ The lower plasma density and temperature means that the plasma thermal current is lower, the sheath is larger, and magnetic field effects may play a significant role. The model discussed in this paper describes the plasma in the vicinity of a hollow-cathode-based plasma contactor that is collecting electrons. Hastings and Blandino⁸ and Iess and Dobrowolny⁹ have presented models of electron-collecting plasma contactors. Their models do not apply to the specific experiments this paper addresses as they assume quasineutrality, i.e., the net charge density is small compared with the ion (or electron) charge density. This excludes the formation of double layers. Potentials and particle densities due to operation of the contactor can be calculated. As the potential determines the sheath area, the collected current can also be computed. The model can be applied with both the laboratory test tank and the space environments. Laboratory results are being used to support the model development. Once the model is validated with laboratory data, it will be used to predict the behavior of similar contactors in space.

The dominant physical processes observed in the laboratory experiments of Wilber and Williams,^{5,6} Patterson,⁷ and others are the formation of a double layer and ionization by the collected electrons. For current collection greater than about 100 mA, contactors are observed to operate in what is known as the ignited mode. In the ignited mode, the plasma plume glows visibly. Within the glowing region, the potential is roughly constant at an elevated potential. At the edge of the glowing region, the potential drops rapidly to nearly zero. This potential drop is accomplished by a plasma double layer, a layer of negative charge and a layer of positive charge.¹⁰ Within the glowing region, two groups of electrons can be distinguished: a Maxwellian component, which has a temperature of 2-3 eV, and a monoenergetic component with an energy given by the double-layer potential difference. The monoenergetic component is composed of those electrons that originated within the ambient plasma and were accelerated as they passed through the double layer. The Maxwellian component is composed of those that were created within the plume. The collected electrons are accelerated by the double layer to energies high enough to excite and ionize the atoms emitted by the contactor, creating the glow. The electrons are then collected by the anode plates. The ions created by this ionization enhance the local plasma density and eventually leave the region, helping to balance the space charge of the collected electrons. Outside of the glowing region, within the ambient

plasma, there are also two components to the electron population: a Maxwellian component with a temperature of 4-8 eV and a lower density monoenergetic component with energy given by the potential difference from the electron source (the simulator hollow cathode) to the ambient plasma. The monoenergetic component is composed of electrons that have not interacted since they left the simulator. The Maxwellian component is composed of simulator electrons that have reached equilibrium with their surroundings. The high background plasma temperature is due to the kinetic energy gained by the acceleration of the simulator electrons as they leave the simulator hollow cathode.

Double-Layer Models

Langmuir¹¹ showed that between two dense quasineutral plasmas at different potentials there is often a region governed by space-charge-limited transport of charge. Such a region is commonly known as a double layer because it consists of a layer of positive charge and a layer of negative charge. Across the double layer, the potential drops sharply. Researchers have been investigating double layers experimentally and theoretically since 1929,¹²⁻¹⁶ but few have previously addressed double layers produced by the spherical expansion of a high-density plasma into a lower-density plasma.

Wei and Wilbur¹⁰ introduced the first model of double layers produced by the expansion of a high-density plasma into another plasma. This model describes spherical double layers as spherical double diodes. A current I_i of ions flows outward from the inner radius r_i , and a current I_o of electrons flows inward from the outer radius r_o . The outer surface is at zero potential, and the inner radius is at ϕ_i . The particles leave each surface in a space-charge-limited manner. All components are assumed to have temperatures small compared with the voltage drop. Given the ratio r_i/r_o and the voltage drop ϕ_i , one can calculate the currents I_o and I_i .

The double diode model is able to order many of the observations and provides insight into the physical phenomena. The success of the model confirms that the plasma forms a double layer. In order to make predictive calculations, a more complex model that includes ionization and temperature effects is needed. In many of the experiments, the maximum potential is only a few times the highest temperature. In order to model these experiments, a finite temperature model that includes the repelled species is needed. In the double diode model, the quasineutral plasma is separated from the double layer by a singularity in the plasma density. The inclusion of temperature removes this singularity. Additionally, a model that uses applied potential, neutral flow rate, and plasma densities and temperatures to calculate the double-layer position and the current collected is desired for space applications.

Theory

The finite temperature model presented here includes the ions and electrons emitted from the contactor, the ions generated by ionization within the contactor plasma, and the charged particles of the background plasma. The inclusion of ionization is crucial to the model's predictive ability. Under most conditions, the I_i ions of the double diode model are almost all created within the volume of the plasma plume. The collected electrons are accelerated by the double layer and ionize the neutrals.

The source plasma is described as being composed of accelerated ions and thermal electrons. Together, the ions and electrons form a quasineutral plasma near the source. The ambient plasma's contribution to the charge density is given by Debye shielding for low potentials. At higher potentials, the charge density decreases due to acceleration of the attracted species. The neutral density has two components. They are the atoms expanding from the contactor and a constant background. The

¹For a flow rate of 4 standard cubic centimeters per minute (sccm) and a tank pressure of 4×10^{-6} T, the neutral density is mostly source neutrals for the first 5 cm from the source and mostly ambient neutrals further out. In space (10^{-7} T), the radius with which the source dominates is 30 cm.

model allows examination of the interaction of the source plasma and the ambient background plasma in detail. The potential and particle number densities are determined by solving Poisson's equation self-consistently with a charge density that includes all of the plasma components

$$-\epsilon_0 \nabla^2 \phi = \rho = e(n_{is} + n_{iz} - n_{es}) + \rho_a \quad (1)$$

The boundary conditions are $\phi = \phi_k$ at a small sphere of size r_{\min} and $\phi = 0$ at the outer boundary of the calculational space. In two- and three-dimensional calculations, additional boundary conditions that describe the anode plates and other objects in the laboratory plasma tank or on a spacecraft can be added.

The contribution of the ambient plasma is taken from an interpolation function¹⁷ for a plasma of temperature θ_a and density n_o :

$$\rho_a(r) = \frac{-en_o \phi(r)/\theta_a}{1 + \sqrt{4\pi \left| \frac{\phi(r)}{\theta_a} \right|^3}} \quad (2)$$

This formula interpolates between the known charge densities at large and small potentials. At small potentials, Debye screening gives the charge density. At large potentials, the charge density is given by the plasma thermal current divided by the velocity of the attracted particles, here electrons. It has been shown to give results that agree with flight data from low-Earth-orbit plasma collection experiments.^{18,19} Figure 2 shows $\rho_a(\phi)$ for normalized parameters. This formula was chosen over others that are based on first principles¹³ because the slope is correct at the origin, the peak charge density occurs at the correct potential, and the formula is more convenient computationally.

Within the plume, Eq. (2) underestimates the contribution of the ambient plasma to the charge density. Geometric convergence of the electrons increases the magnitude of the charge density. Because ρ_a/ρ is small within the plume, ignoring convergence in the calculation of the charge density does not significantly affect calculational results for laboratory contactors. The validity of this estimate must be verified for each calculation. Because the potential in these calculations is positive, ρ_a is negative and, therefore, represents an excess of electrons over ions.

The source is a sector of a spherical surface with solid angle Ω and radius r_{\min} at potential ϕ_k that emits an ion current I_i of ions with kinetic energy E and mass m_{hc} . The plasma source

ions are accelerating and expanding. When spherical symmetry is assumed, the source ion number density is given by

$$n_{is}(r) = n_i^o \left(\frac{r_{\min}}{r} \right)^2 \sqrt{\frac{E}{E + \phi_k - \phi(r)}} \quad (3)$$

where

$$n_i^o = \frac{I_i}{e\Omega r_{\min}^2 \sqrt{2eE/m_{hc}}} \quad (4)$$

When spherical symmetry does not describe the experiment adequately, $n_{is}(r)$ can be determined by particle tracking or hydrodynamic techniques.

The plasma source electrons are assumed to have a Boltzmann distribution of energies with temperature θ . Their number density is given by

$$n_{es}(r) = n_{es}^o (e^{\phi(r)/\theta} - 1) \quad (5)$$

The -1 is included so that the number density is zero for zero potential. With this expression, the total charge density at zero potential and infinite radius is zero. The value of n_{es}^o is chosen so that the net charge density is nearly zero throughout the plume.

The rate of ion creation is given by

$$\dot{n}_{iz}(r, \phi, \theta_a) = \sigma(\phi + \theta_a) n_e(r) n_e(r) v_e(\phi + \theta_a) \quad (6)$$

The electron velocity and the ionization cross section²⁰ σ depend on the kinetic energy of the accelerated electrons. In the spherically symmetric case,

$$n_{iz}(r) = \int_{r_{\min}}^r \frac{r_1^2}{r^2} \frac{\dot{n}_{iz}[r_1, \phi(r_1), \theta_a]}{\sqrt{2e[E_1 + \phi(r_1) - \phi(r)]/m_{hc}}} dr_1 \quad (7)$$

When spherical symmetry is not assumed, $n_{iz}(r)$ is no longer a simple integral.

The density of neutrals has two components. There is the contribution from the ambient pressure and the contribution from the atoms expanding from the cathode. As long as the fraction of gas ionized is small, the density of atoms emitted by the contactor is assumed to vary inversely with the distance squared and to have a cosine dependence on angle,

$$n_n(r) = n_{no} + \dot{n} \frac{1}{\Omega r^2 v_n} 2 \cos \Psi \quad (8)$$

where Ψ is the angle between r and the line of axial symmetry of the contactor. When spherical symmetry is assumed, the $2\cos\Psi$ factor is omitted. The flow rate of atoms leaving the contactor is an experimental quantity. The velocity of expansion is given by Shapiro²¹:

$$v_n = \sqrt{\frac{5e\theta_n}{m_{hc}}} \quad (9)$$

The density of accelerated electrons within the plume is the primary factor determining n_{iz} . Thus, an accurate treatment, including geometric convergence, is needed. Naively, one might assume that with spherical symmetry the position dependence of the density of accelerated electrons would be given by $1/r^2$. However, the electron density variation seen in the experiments is less dramatic than that given by r^2 . In the laboratory experiments, the temperature of the ambient environment can be 20% of the potential drop across the double layer. The high thermal component of the electron energy means that the angular momentum of the incoming electrons must be included when computing the electron density. The electron density for a spherical square well potential, assuming a Maxwellian dis-

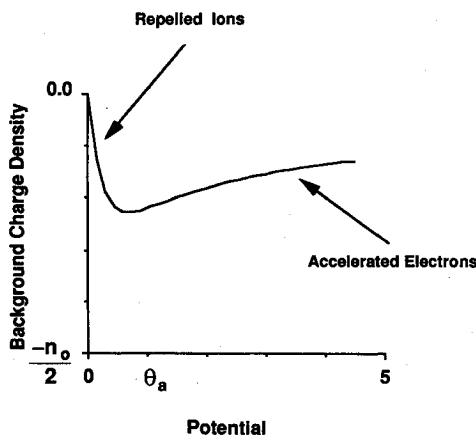


Fig. 2 Ambient plasma charge density as a function of potential for positive potentials; plasma temperature and Debye length are taken to be 1.

tribution of electrons at infinity and conserving angular momentum, is given by

$$\frac{n_o}{\sqrt{\pi}} \left\{ \frac{\sqrt{\pi}}{2} \exp[\phi/\theta_a] [1 - \operatorname{erf}(\sqrt{\phi/\theta_a})] + \sqrt{\frac{a^2}{r^2} - 1} \exp\left[\frac{-\phi/\theta_a}{a^2/r^2 - 1}\right] \int_0^{\sqrt{\frac{\phi/\theta_a}{a^2/r^2 - 1}}} \exp[y^2] dy \right\} \quad (10)$$

The inclusion of angular momentum dramatically reduces the peak electron density compared to the peak obtained when angular momentum is ignored. Figure 3 illustrates the difference in electron density estimates with and without angular momentum for a spherical square well of depth $5\theta_a$. The peak collected electron density from Eq. 10 is given by

$$n_e(0) = n_a \left\{ \frac{1}{\sqrt{\pi}} \sqrt{\frac{\phi_k}{\theta_a}} + \frac{1}{2\sqrt{\pi}} \sqrt{\frac{\theta_a}{\phi_k}} + \mathcal{O} \left[\left(\frac{\phi_k}{\theta_a} \right)^{-3/2} \right] \right\} \quad (11)$$

For one-dimensional computations, $n_e(r, \phi)$ for the double layer problem is approximated by $n_e(r)$ for a spherical square well within a radius equal to the radius of the center of the double layer and depth ϕ .

A plasma, with the components that were just described, can form a double layer if ϕ_k is large enough. Katz and Davis²² relate the presence and location of the double layer to roots of the charge density equation. Within the source plasma plume, the charge density has a single root near ϕ_k . Within the ambient plasma, the charge density has a single root near zero. Within the double layer, the charge density has three roots. The plasma potential adjusts so that the potential is near the upper root at the inner edge of the double layer and near the lower root at the outer edge. In order for the potential to be continuous, the plasma cannot be quasineutral throughout the double layer, leading to charge separation in that region.

Calculations

The model just described has been incorporated into a spherically symmetric computer code called DOUBLE. It uses an iterative scheme. DOUBLE provides only an estimate of behavior for contactors for which the size of the anode plates is comparable to the sheath size. Codes that solve the previous equations without the constraint of spherical symmetry are needed to examine the two- and three-dimensional effects. DOUBLE runs quickly (1/2 h on a Sun 3 workstation) and, therefore, can be used to extensively examine the parameter

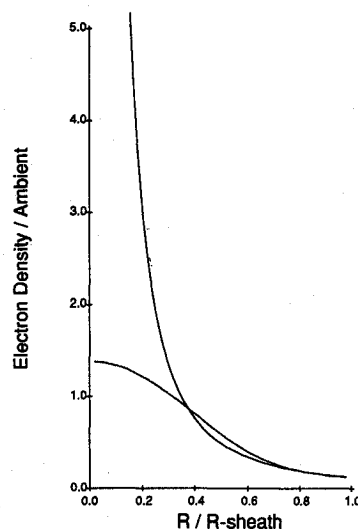


Fig. 3 Comparison of electron density as a function of radius for spherical square well of potential depth $5\theta_a$ with (nondivergent curve) and without (divergent curve) consideration of angular momentum.

dependencies of the model. Both approaches are needed to obtain a complete characterization of the model. Only the results of spherically symmetric calculations are presented here.

For the calculation results that follow, we chose parameters from a single operating point experiment done by Williams and Wilbur.²³ The results agree well enough to confirm that the primary physical effects present in the experiments are present in the model.

Figures 4 compare the results of a spherically symmetric calculation with the corresponding experimental results. The expellant gas used is xenon. The ambient pressure used is the measured value of 3.4×10^{-6} T. The computational space is a 2π steradian sector of spherical space with radius extending from 0.15 to 30 cm. The inner and outer radius boundary conditions are at a fixed potential. The outer boundary is taken to be at 0 V. The potential at the inner boundary in the calculations, 40 V, is higher than the 32 V potential actually applied to the keeper ring (and anode plates) in the experiments. The ambient density and temperature are the experimentally measured values of $1.8 \times 10^{13} \text{ m}^{-3}$ and 7.5 eV. All of the ion current flowing away from the contactor is assumed to be generated by ionization within the confines of the grid so that the ion current from the source is zero. The density and temperature of electrons from the source are determined by a fit to the measured values. The source temperature is 3.5 eV and the density coefficient n_{e0}^2 , used in Eq. (5), is $6 \times 10^9 \text{ m}^{-3}$. This choice gives a source electron density of $3 \times 10^{13} \text{ m}^{-3}$ when the potential is 30 V. The energy of the ions immediately after ionization is chosen to be 0.1 eV. (The results do not depend on this parameter as long as it is less than 1 eV.)

As is discussed later, this calculation underestimates the density of the ambient electrons within the plume. The ionization rate is proportional to the product of the gas density and the ambient electron density within the plume. Therefore, in order to generate enough ions to sustain the double layer in the measured position, an elevated flow rate must be used in the calculations. The actual flow rate is 4.1 sccm; the value used in the calculation is 7.6 sccm.

The calculated curves and measured values shown in Figs. 4 are generally consistent with each other. Other than plasma measurements within the plume, the experimental numbers are valid to 10%. Within the plume, experimental plasma values are only valid to 50%. In Fig. 4a, the sharp drop in potential at the double layer occurs at the same radius in both experiment and theory. The computational boundary difficulties associated with spherical symmetry and the anode sheath introduce a fictitious sharp rise in potential at the minimum radius.

The curve in which experiment and theory do not agree is Fig. 4b for the density of the ambient electrons. The differences between calculation and experiment can be attributed to several factors, both theoretical and experimental. Two major effects that enhance the electron density are not included in this calculation. Trapped particles due to asymmetries in the potential lead to an enhancement of the electron density, particularly at the edge of the plume where slow electrons are reflected. Another significant effect that is not included in the calculation is presheath current enhancement.²⁴ The inclusion of the presheath effect would lead to an increase in electron density of at least 50%. When comparing the measured and computed curves, it is also necessary to consider the difficulties inherent in the measurement of the plasma properties. Langmuir probe measurements in the plume region are very difficult to interpret because of the high density of monoenergetic electrons. The trend observed in the measurements is that the monoenergetic component of the electron density within the plume is greater than the density of the Maxwellian component in the ambient region. The density of the monoenergetic component increases near the contactor; the ambient electrons undergo some convergence. The scatter observed in the plotted experimental data is indicative of the difficulties associated with this density measurement.

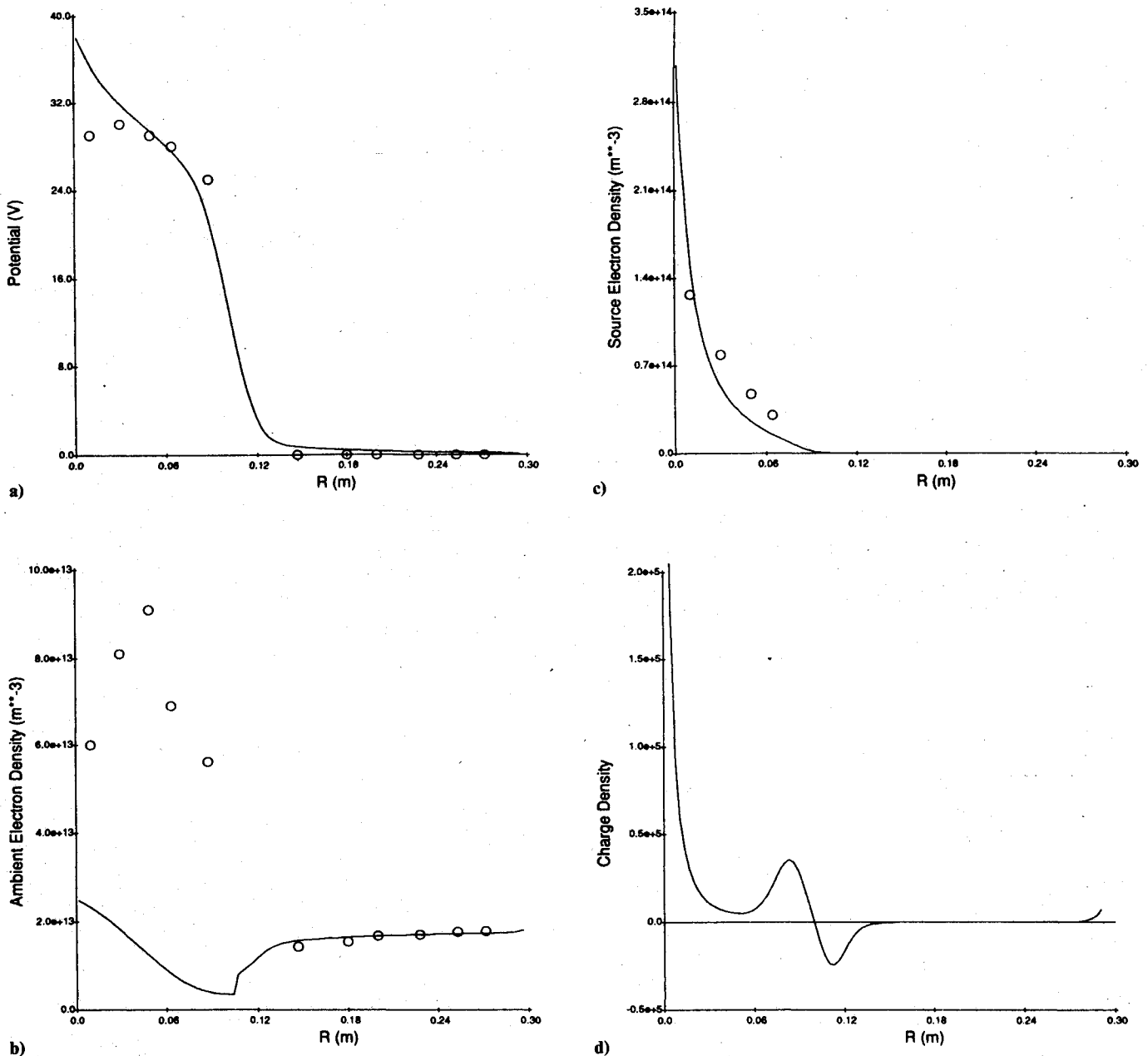


Fig. 4 Comparison of calculation and experiment. The circles are measurements made by Williams and Wilbur²³: a) potential; b) ambient electron density; c) source electron density; d) net charge density.

The close agreement in source electron density seen in Fig. 4c indicates that all of the significant contributions to the charge density within the plume are included in the calculations. These electrons provide the charge density needed to maintain quasineutrality within the plume. Only very near the source do the source electrons dominate the electron population. Figure 4d shows the net charge density. The plasma is clearly quasineutral throughout most of the computational space. The double layer of charge density extending from 7 to 13 cm is clearly visible. Outside the double layer, the plasma is quasineutral. The center of the double layer occurs at the location predicted by Ref. 22. At a higher plasma density, the double layer would be thinner. The enhanced charge density at small radii is an artifact of the calculational method.

The collected current is the product of the collecting area and the thermal current. The collecting area is taken to be the surface with potential $0.7 \theta_a$. The collected electron current for this calculation is 120 mA. The emitted ion current is 0.25 mA. Inclusion of the presheath factor²⁴ elevates the current collected to 180 mA. The measured collected current is 350 mA.

This factor of two difference is consistent with the difference between the measured and calculated ambient electron density.

Figure 5 shows how the collected current varies with plasma density. The parameters used to create this curve are the same as in Figs. 4 with the exception of the ambient plasma density. A linear relationship between the current collected and the ambient plasma density has been observed in the laboratory when the potential was held nearly constant.²⁵ The relationship is almost linear because the sheath area does not change with ambient plasma density and the thermal current varies linearly with plasma density. The amount of ionization that occurs varies linearly with converging electron density. The two competing effects of more ionization and an increase in ambient plasma density cancel so that the double layer location does not change significantly.

Figure 6 shows the calculated current voltage characteristic. The parameters used to create this curve are the same as in Figs. 4 with the exception of the potential. The effective resistance drops from 1600 Ω at 25 V to 140 Ω at 55 V with a value of 340 Ω at 40 V. The current rises steeply, as seen in many of

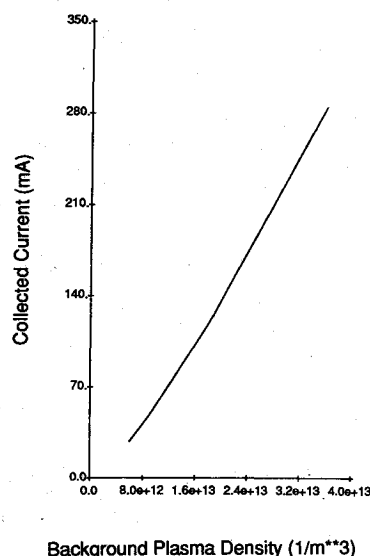


Fig. 5 Collected current as a function of ambient plasma density.

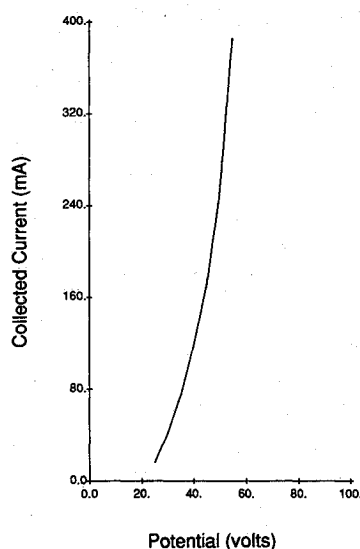


Fig. 6 Collected current as a function of keeper potential.

the contactor experiments. An increase in voltage results in an increase in the cross section for ionization. The additional ions expand the double layer, which increases the collection area.

Conclusions

The model described here can provide numerical estimates of the behavior of plasma contactors in the laboratory. The success of the model confirms the presence of a double layer surrounding the high-density plasma plume. Ionization throughout the plasma plume provides the ions that leave the plume. The high currents and small double-layer radii seen in the laboratory correspond to high background plasma densities. Comparison between calculation and measurement suggests that the major physical interactions are included. The theory is valid for those potentials, temperatures, and densities at which enough ionization occurs to create a quasineutral source plasma and not enough ionization occurs to deplete the neutral density. The differences between the theoretical and experimental results may be due to a combination of factors including experimental geometry, presheath convergence, electron trapping, and electron source-contactor interactions.

These and other issues will be addressed in future work with the use of two- and three-dimensional computer codes.

This model, with modifications, will allow predictions to be made about the behavior of similar contactors in space. The different environment of space will lead to different contactor characteristics. For example, the plasma thermal current is much lower in space so that the plasma plume must be larger. With a larger collecting area, the earth's magnetic fields may restrict collection. Computer modeling does not take the place of space experiments such as HOCAT (hollow cathode sounding rocket experiment)²⁶ but can be used as a guide during experiment design and as an aid to interpretation of results. Computer models can also be used to indicate the effect that the presence of a plasma contactor will have on other instrumentation on a spacecraft.

Acknowledgments

This work was supported by NASA Lewis Research Center under Contract NAS3-23881. The authors benefited from the free and open exchange of data with Paul Wilbur and John Williams of Colorado State University and Michael Patterson of NASA Lewis Research Center. This interchange occurred as part of an investigative program under the direction of Joseph Kolecki of NASA Lewis Research Center. The authors thank the reviewers for their helpful comments.

References

- ¹Patterson, M. J., and Wilbur, P. J., "Plasma Contactors for Electrodynamical Tethers," *Advances in the Astronautical Sciences*, edited by P. M. Bainum, I. Bekey, L. Guerriero, and P. A. Penzo, Vol. 62, Univelt, San Diego, CA, 1986, pp. 383-405.
- ²Sasaki, S. et al., "Neutralization of Beam-Emitting Spacecraft by Plasma Injection," *Journal of Spacecraft and Rockets*, Vol. 24, No. 3, 1987, pp. 227-231.
- ³Olsen, R. C., "Modification of Spacecraft Potentials by Plasma Emission," *Journal of Spacecraft and Rockets*, Vol. 18, No. 5, 1981, pp. 462-469.
- ⁴Purvis, C., "OTEP—A Vision for the Future," AIAA Paper 89-0682, Jan. 1989.
- ⁵Wilbur, P. J., and Williams, J. D., "An Experimental Investigation of the Plasma Contacting Process," AIAA Paper 87-0571, Jan. 1987.
- ⁶Williams, J. D., and Wilbur, P. J., "Plasma Contacting—An Enabling Technology," AIAA Paper 89-0677, Jan. 1989.
- ⁷Patterson, M. J., "Hollow Cathode-Based Plasma Contactor Experiments for Electrodynamical Tether," AIAA Paper 87-0571, Jan. 1987.
- ⁸Hastings, D. E., and Blandino, J., "Bounds on Current Collection from the Far Field by Plasma Clouds in the Ionosphere," *Journal of Geophysical Research*, Vol. 94, No. A3, 1989, pp. 2737-2744.
- ⁹Jess, L., and Dobrowolny, M., "The Interaction of a Hollow Cathode with the Ionosphere," *Physics of Fluids B*, Vol. 1, No. 9, 1989, pp. 1880-1889.
- ¹⁰Wei, R., and Wilbur, P. J., "Space-Charge-Limited Current Flow in a Spherical Double Sheath," *Journal of Applied Physics*, Vol. 60, No. 7, 1986, pp. 2280-2284.
- ¹¹Langmuir, I., "The Interaction of Electron and Positive Ion Space Charges in Cathode Sheaths," *Physical Review*, Vol. 33, No. 6, 1929, pp. 954-989.
- ¹²Andersson, D., and Sørensen, J., "Numerical Double Layer Solutions with Ionisation," *Journal of Physics D: Applied Physics*, Vol. 16, 1983, pp. 601-611.
- ¹³Andrews, J. G., and Allen, J. E., "Theory of a Double Sheath Between Two Plasmas," *Proceedings of the Royal Society of London A*, Vol. 320, 1971, pp. 459-472.
- ¹⁴Block, L. P., "A Double Layer Review," *Astrophysics and Space Science*, Vol. 55, 1978, pp. 59-83.
- ¹⁵Knorr, G., and Goertz, C. K., "Existence and Stability of Strong Potential Double Layers," *Astrophysics and Space Science*, Vol. 31, 1974, pp. 209-223.
- ¹⁶Schamel, H., and Bujarbarua, S., "Analytical Double Layers," *Physics of Fluids*, Vol. 26, No. 1, 1983, pp. 190-193.
- ¹⁷Katz, I., Mandell, M. J., Schnuelle, G. W., Parks, D. E., and Steen, P. G., "Plasma Collection by High-Voltage Spacecraft at Low Earth Orbit," *Journal of Spacecraft and Rockets*, Vol. 18, No. 1, 1981, pp. 79-82.

¹⁸Mandell, M. J., Katz, I., and Cooke, D. L., "Potentials on Large Spacecraft in LEO," *IEEE Transactions on Nuclear Science*, Vol. NS-29, No. 6, 1982, pp. 1584-1588.

¹⁹Katz, I. et al., "Structure of the Bipolar Plasma Sheath Generated by SPEAR I," *Journal of Geophysical Research*, Vol. 94, No. A2, 1989, pp. 1450-1458.

²⁰Rapp, D., and Englander-Golden, P., "Total Cross Sections for Ionization and Attachment in Gases by Electron Impact. I. Positive Ionization," *Journal of Chemical Physics*, Vol. 43, No. 5, 1965, pp. 1464-1479.

²¹Shapiro, A. H., *The Dynamics and Thermodynamics of Compressible Fluid Flow*, Vol. 1, Ronald Press, New York, 1953, p. 79.

²²Katz, I., and Davis, V. A., "A Van der Waal's Like Theory of

Plasma Double Layers," *Physics of Fluids B*, Vol. 1, No. 10, 1989, pp. 2121-2125.

²³Williams, J., and Wilbur, P., private communications, Dec. 1988.

²⁴Parrot, M. J. M., Storey, L. R. O., Parker, L. W., and Laframboise, J. G., "Theory of Cylindrical and Spherical Langmuir Probes in the Limit of Vanishing Debye Number," *Physics of Fluids*, Vol. 25, No. 12, 1982, pp. 2388-2400.

²⁵Wilbur, P., and Williams, J., private communications, Nov. 1988.

²⁶Olsen, R. C., "HOCAT—A Sounding Rocket Borne Plasma Contactor Experiment," AIAA Paper 89-0680, Jan. 1989.

Henry B. Garrett
Associate Editor

*Recommended Reading from the AIAA
Progress in Astronautics and Aeronautics Series . . .*



Thermal Design of Aeroassisted Orbital Transfer Vehicles

H. F. Nelson, editor

Underscoring the importance of sound thermophysical knowledge in spacecraft design, this volume emphasizes effective use of numerical analysis and presents recent advances and current thinking about the design of aeroassisted orbital transfer vehicles (AOTVs). Its 22 chapters cover flow field analysis, trajectories (including impact of atmospheric uncertainties and viscous interaction effects), thermal protection, and surface effects such as temperature-dependent reaction rate expressions for oxygen recombination; surface-ship equations for low-Reynolds-number multicomponent air flow, rate chemistry in flight regimes, and noncatalytic surfaces for metallic heat shields.

TO ORDER: Write, Phone or FAX:

American Institute of Aeronautics and Astronautics,
c/o TASC0, 9 Jay Gould Ct., P.O. Box 753, Waldorf, MD 20604
Phone (301) 645-5643, Dept. 415 • FAX (301) 843-0159

Sales Tax: CA residents, 7%; DC, 6%. For shipping and handling add \$4.75 for 1-4 books (call for rates for higher quantities). Orders under \$50.00 must be prepaid. Foreign orders must be prepaid. Please allow 4 weeks for delivery. Prices are subject to change without notice. Returns will be accepted within 15 days.

1985 566 pp., illus. Hardback
ISBN 0-915928-94-9
AIAA Members \$54.95
Nonmembers \$81.95
Order Number V-96